

Spin and spectral signatures of polaron pairs in π -conjugated polymers

P. A. Lane,^{*} X. Wei,[†] and Z. V. Vardeny

Department of Physics, University of Utah, Salt Lake City, Utah 84112

(Received 3 March 1997)

We have studied polaron pair photoexcitations in a variety of π -conjugated polymer films by photoinduced absorption (PA) and optically detected magnetic resonance (ODMR). Both luminescent and nonluminescent polymers have been studied. An exchange interaction between polarons broadens their magnetic resonance spectrum, permitting the unambiguous identification of the polaron pair species by ODMR. Both isotropic and anisotropic exchange interactions have been observed. An isotropic exchange interaction broadens the spin- $\frac{1}{2}$ resonance associated with polarons, whereas an anisotropic exchange interaction gives rise to both full-field and half-field powder patterns. We have successfully modeled the observed spin- $\frac{1}{2}$ ODMR spectra and estimate the strength of the isotropic exchange interaction J . An anisotropic exchange interaction has been observed in C₆₀-doped 2,5-dioctyloxy poly(*p*-phenylene vinylene) and cis-rich polyacetylene. Both polarons and polaron pairs are characterized by two absorption bands. However, the high-energy PA band of polaron pairs is blueshifted with respect to that of isolated polarons and the low-energy PA band of polaron pairs is relatively weak. We have also observed neutral soliton pair excitations in polymers with degenerate ground states. [S0163-1829(97)03131-7]

I. INTRODUCTION

The initial report of electroluminescence from poly(*p*-phenylene vinylene) (PPV) thin films has stimulated¹ extensive studies of the radiative and nonradiative decay processes of π -conjugated polymers.² For both practical and theoretical reasons, decay processes that affect the radiative quantum yield η are of great interest. The primary photoexcitations in π -conjugated polymers are intrachain singlet excitons, formed with nearly unit quantum yield^{3,4} and having binding energies of a few tenths of an eV.⁵⁻⁷ The exciton thermalizes within 1 ps by relaxation in the polymer chain followed by migration to chain segments with the lowest energy (longest conjugation).⁸⁻¹⁰ Excitons can decay by light emission [photoluminescence (PL)], intersystem crossing to form triplet excitons (which decay nonradiatively), and possibly interchain charge transfer leading to the formation of polarons and/or Coulomb-correlated polaron pairs.¹¹⁻¹³



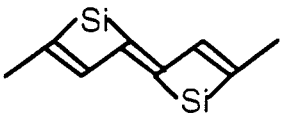
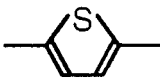
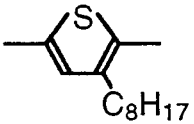
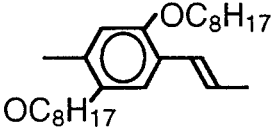
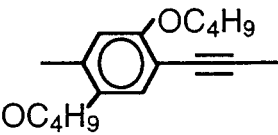
The PL efficiency η of polymer films is significantly lower than that of solutions or dilute blends with inert polymers.¹⁴ The drop in η is accompanied by changes in fast (ps) photoexcitation dynamics; the PL of solutions and blends of PPV derivatives decays nearly exponentially, whereas the PL of most films exhibits nonexponential decay with long-lived components.¹² These observations have led to suggestions that interchain polaron pairs bound by Coulomb attraction are the primary photoexcitations in polymer films.^{11,12} Much speculation has focused on the transient photomodulation (PM) spectra, which contain both stimulated emission and photoinduced absorption (PA) bands. The difficulty in identifying polaron pair photoexcitations lies in the complexity of PM spectra. The PA bands in the visible spectral range have been assigned to excitons, polarons, or polaron pairs. In the ps time domain, the existence of electronic states with energies above the gap gives rise to PA bands with dynamics matching those of the PL.¹⁵ Moreover, triplet excitons and polarons may also contribute to the PM

spectrum. Similar difficulties exist in the analysis of the steady-state (ms) PM spectra. Hence, arguments regarding assignment of the PM spectra have been indirect.

In this paper we present a study of polaron pairs in π -conjugated polymer films using PA, PA-detected magnetic resonance (PADMR), and PL-detected magnetic resonance (PLDMR). PADMR combines the advantages of PA (spectral information) and electron spin resonance (spin selectivity) and is thus ideally suited to investigate polaron pair photoexcitations. Studies of the magnetic field effect on the photoconductivity of π -conjugated polymer films have led Frankevich *et al.*¹⁶ to suggest that exchange coupling between polarons plays a significant role in the dissociation of pairs to create charge carriers. The exchange interaction results from a coupling of the spatial coordinates of an ion (polaron) pair to their spins.¹⁷ When a pair of electrons forms a bond between two atoms, the result is a spin singlet state as the two electrons must pair their spins to obey the Pauli principle. If the bond is strong, the possibility of having the two electrons with parallel spins is very low since the triplet state has a much higher energy than the singlet. If, however, the bonding energy is weak, then the spacing of the energy levels is much closer. While the exchange interaction depends upon the coordinates of the electrons forming the pair, the complete wave function of the system must be antisymmetric with respect to electron exchange. Hence, the orbital and spin functions are coupled and the spins act as indicators of the nature of the orbital states. The observation of an exchange effect is significant as this interaction modifies the magnetic resonance spectra of polaron pairs, but not that of isolated or loosely correlated polarons. PADMR can thus be used to identify polaron pairs and measure their PA spectra.

This paper has the following outline. We first show experimental evidence (via PADMR and PLDMR) for a spin-exchange interaction between polarons composing Coulomb-bound polaron pairs. These magnetic resonance spectra have been successfully modeled by either isotropic or anisotropic

TABLE I. Summary of polymers and their optical properties. Data on *trans*-(CH)_x and *cis*-rich (CD)_x taken from Ref. 9; *e*-PT from Ref. 20; P3OT from Ref. 21; PDES and DBO-PPE from Ref. 22.

| Polymer | Repeat Unit | Ground state | Soluble? | η | E_{gap} |
|------------------------------------|---|---------------|----------|------------------|------------------|
| <i>trans</i> -(CH) _x |  | Degenerate | No | 10 ⁻⁵ | 1.4 eV |
| <i>cis</i> -rich (CD) _x |  | Both | No | 10 ⁻³ | 1.5 eV |
| PDES |  | Nondegenerate | Yes | 10 ⁻⁵ | 1.8 eV |
| <i>e</i> -PT |  | Nondegenerate | No | 10 ⁻³ | 2.0 eV |
| P3OT |  | Nondegenerate | Yes | 0.15 | 2.0 eV |
| DOO-PPV |  | Nondegenerate | Yes | 0.24 | 2.2 eV |
| DBO-PPE |  | Nondegenerate | Yes | 0.15 | 2.5 eV |

exchange interactions. We then use λ PADMR spectroscopy to measure the PA spectra of polaron pairs; the polaron pair species is characterized by two PA bands. The higher-energy PA band of polaron pairs occurs at a higher energy than the corresponding band of isolated polarons and is much stronger than the lower-energy polaron pair PA band. We also show evidence for neutral soliton pair excitations in *trans*-polyacetylene.

II. MATERIALS AND EXPERIMENTAL TECHNIQUES

We have studied the following π -conjugated polymers (Table I), which encompass a broad variety of photophysical properties: *trans*-polyacetylene [*trans*-(CH)_x], deuterated *cis*-rich polyacetylene [*cis*-rich (CD)_x], poly(diethynylsilane) (PDES), electrochemically polymerized polythiophene (*e*-PT), poly(3-octyl thiophene) (P3OT), 2,5-dioctyloxy poly(*p*-phenylene vinylene) (DOO-PPV), and 2,5-dibutoxy poly(*p*-phenylene ethynylene) (DBO-PPE). We also measured C₆₀-doped films of P3OT, DOO-PPV, and DBO-PPE. These films include polymers with both degenerate (DGS) and nondegenerate (NDGS) ground states and with PL quan-

tum yields varying from 10⁻⁴ to 0.24.¹⁹⁻²² The polyacetylene samples were polymerized by the Shirakawa method. The *cis*-rich (CD)_x sample contains both *cis* and *trans* segments. The relative positions of the lowest excited odd ($1B_u$) and even ($2A_g$) parity excited states determines whether or not a conjugated polymer is luminescent.¹⁵ However, *e*-PT films are only weakly luminescent due to a high density of defects. All samples measured are thin films either cast from solutions onto sapphire substrates or directly polymerized onto the substrates. For fullerene-doped films, C₆₀ was purchased¹⁸ and dissolved with the polymer in solution before the film was cast.

A schematic diagram of the PA and PADMR spectrometers used in this study is shown in Fig. 1.²³ PA spectroscopy uses two beams; a pump beam produces the excited states and the probe beam measures the changes ΔT in the transmission T . The sample is placed in a cold-finger cryostat and excited by a pump beam from an Ar⁺ laser. PL from the sample or transmitted light from the probe beam is dispersed through a $\frac{1}{4}$ -m monochromator onto a photodiode. By the use of multiple monochromator gratings and IR detectors, we could measure PA in the spectral range from 0.1 to 3.5 eV. The normalized changes in transmission $-\Delta T/T \approx n\sigma d$,

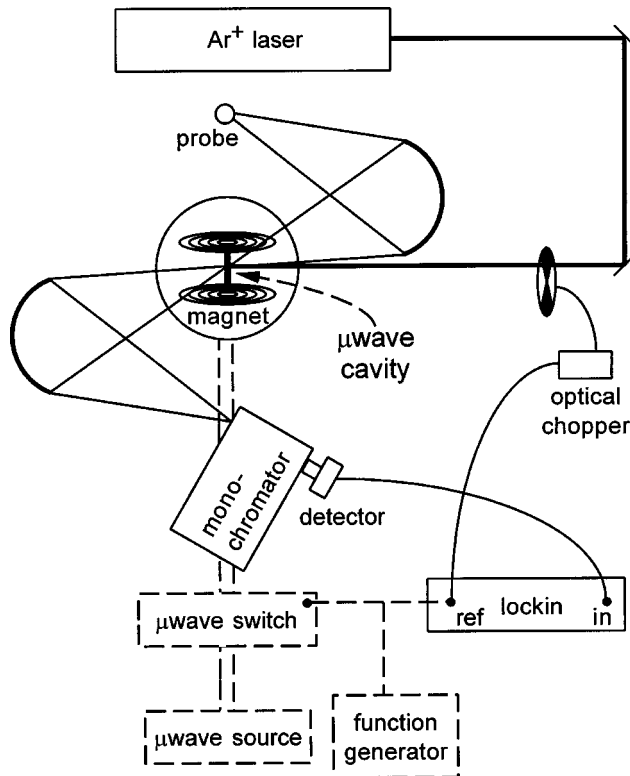


FIG. 1. Schematic diagram of the PA and ODMR spectrometers. The microwave apparatus used for ODMR is shown with a dashed line.

where n is the photoexcitation density, σ is the IR absorption cross section, and d is the sample thickness. The pump beam is chopped by an acousto-optic modulator and the use of standard phase-sensitive lock-in techniques yields a signal resolution as low as 10^{-6} . In a typical experiment, the absorbed flux from the laser is about 2×10^{18} photons/cm² sec at $\hbar\omega_{\text{pump}} = 2.54$ eV.

Since its introduction in 1967,^{24,25} optically detected magnetic resonance (ODMR) has been successfully applied to a variety of systems. As excited-state recombination is a spin-dependent process, resonant absorption of microwaves redistributes excited-state populations among the magnetic substrates. This, in turn, enhances or diminishes the recombination rate of the excited states, resulting in a change in optical properties (emission or absorption) associated with these states. The advantage of ODMR over conventional electron spin resonance (ESR) is that the detection energy is scaled up from the microwave region to the near IR and visible spectral ranges, which makes ODMR up to 10^5 times more sensitive than ESR. ODMR has been most commonly applied to detect changes in PL (PLDMR) and more recently extended to changes in PA (PADMR).²⁶ Whereas PLDMR can be applied only to luminescent systems, no similar limitation exists for PADMR. Furthermore, PLDMR can provide only limited spectral information. In π -conjugated polymers, the excitations detected by ODMR (Ref. 27) recombine non-radiatively and only affect the PL indirectly (either by quenching singlet excitons or through ground-state recovery²⁸). Hence, the spectral dependence of the PLDMR signal usually mirrors the PL spectrum.²⁸ However, these excitations have distinct PA signals, which can be measured

by fixing the magnetic field on resonance and scanning the probe wavelength λ . We present both H -PADMR (swept magnetic field at fixed probe λ) and λ -PADMR (swept probe wavelength at fixed H) measurements.

The ODMR spectrometer²⁸ consists of the regular PA apparatus with the sample mounted in a high- Q microwave cavity equipped with optical windows and a superconducting magnet with field H . 3-GHz microwaves are produced by a Klystron generator, modulated by a pin-switch diode, and then introduced into the cavity through a coaxial waveguide. The entire apparatus is contained within a liquid-helium cryostat; measurements were performed below 10 K. Magnetic resonance occurs when the Zeeman energy splitting of two levels is equal to the energy of a microwave photon, causing transitions between magnetic sublevels due to resonant absorption (or emission) of microwaves. As these transitions tend to equalize the populations of the two coupled levels, magnetic resonance requires that the populations of the levels be unequal; i.e., the spin polarization is nonzero. Unlike ESR, ODMR is a dynamic technique that is not based on spin states in thermal equilibrium. Hence, in order to detect an ODMR signal, we must actively provide spin polarization. This can be achieved during the generation and recombination processes.

For pairs of spin- $\frac{1}{2}$ particles, we can quantitatively describe the spin polarization. Consider parallel (P) and anti-parallel (AP) pairs with respective generation and recombination rates G_i and R_i . The steady-state densities in the absence of microwaves are given by $n_i = G_i/R_i$. Under saturation by microwaves on resonance, the two levels are coupled: $n_P = n_{AP} = \tilde{n}$, where $\tilde{n} = (G_P + G_{AP})/(R_P + R_{AP})$.²⁸ For PADMR, the signal measured is proportional to the normalized change in the excitation density $\delta n/n$, which can be calculated from the above relations:

$$\frac{\delta n}{n} = \frac{\Delta n}{n} \frac{\Delta R}{R}, \quad (1)$$

where $\Delta n = n_{AP} - n_P$ with no microwaves and $\Delta R = R_{AP} - R_P$. The recombination rate of antiparallel pairs always exceeds the rate of parallel pairs, giving $\Delta R > 0$.

When calculating the spin polarization for pairs of spin- $\frac{1}{2}$ excitations, we first consider the case of a geminate pair, i.e., a pair that is formed together. As the ground state of π -conjugated polymers is spin singlet and photon absorption conserves spin, the photogenerated pair will be in an antiparallel spin state. Spin polarization is thus achieved by generation; microwave absorption flips the spin of one carrier, reducing the recombination rate of the pair to the ground state. Magnetic resonance would result in a positive PADMR ($-\delta T/T > 0$) and negative PLDMR ($\delta I/I < 0$).²⁸ For visible excitation of conjugated polymers, the spin- $\frac{1}{2}$ ODMR signals have been of the opposite sign²⁶ (requiring $\delta n/n < 0$) and thus cannot be attributed to geminate pairs. Rather, these signals must be due to either nongeminate pairs or long-lived pairs whose spins have evolved through hyperfine or exchange interactions.

Nongeminate pairs are formed from two polarons resulting from completely dissociated excitons. The spins of the polarons will be randomly oriented, leading to equal generation rates for both kinds of pairs ($G_P = G_{AP}$) and $\delta n/n =$

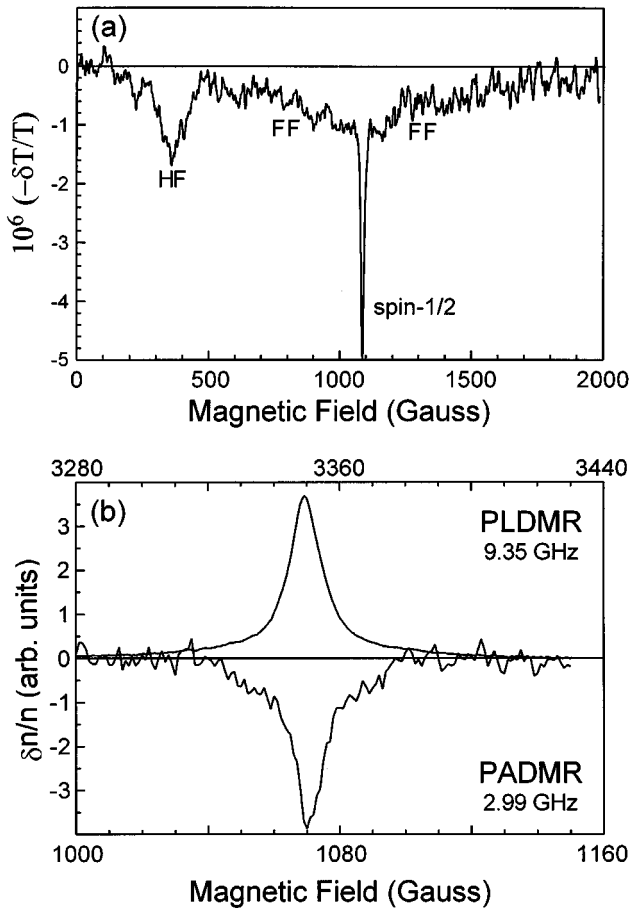


FIG. 2. (a) H -PADMR spectrum of DBO-PPE film from 0 to 2 kG. (b) H -PLDMR and H -PADMR spectra of the polaron pair resonance at $g \approx 2$.

$-\left[\Delta R/(R_{AP} + R_P)\right]^2$. The sign of this resonance agrees with previously observed ODMR spectra of polarons in conjugated polymers.^{26–28} Analysis of spin-correlated polaron pairs is more complicated. The eigenfunctions of the spin exchange Hamiltonian are pairs with quantum numbers S , m_S , S_1 , and S_2 , with one $S=0$ “singlet” solution and three $S=1$ “triplet” solutions. The spin exchange Hamiltonian and its associated magnetic resonance spectra are analyzed in detail below.

III. SPIN SIGNATURE OF EXCHANGE-CORRELATED POLARON PAIRS

A. Experiment

The H -PADMR spectrum of DBO-PPE, measured at a probe photon energy of 1.6 eV, is shown in Fig. 2(a). The $S=1$ magnetic resonance spectrum of the triplet excitons consists a 1000-G-wide “full-field” (FF) powder pattern centered at 1070 G and a narrow, “half-field” (HF) powder pattern at $H=380$ G. The spin- $\frac{1}{2}$ PLDMR (Ref. 29) and H -PADMR spectra [Fig. 2(b)] consist of a narrow Gaussian line [full width at half maximum (FWHM) of 12 G] superimposed upon a broad (~ 70 G wide) resonance line. The two lines are correlated as they have the same dependence on temperature and microwave power; they also have the same λ -PADMR spectrum (see below). No half-field resonance is

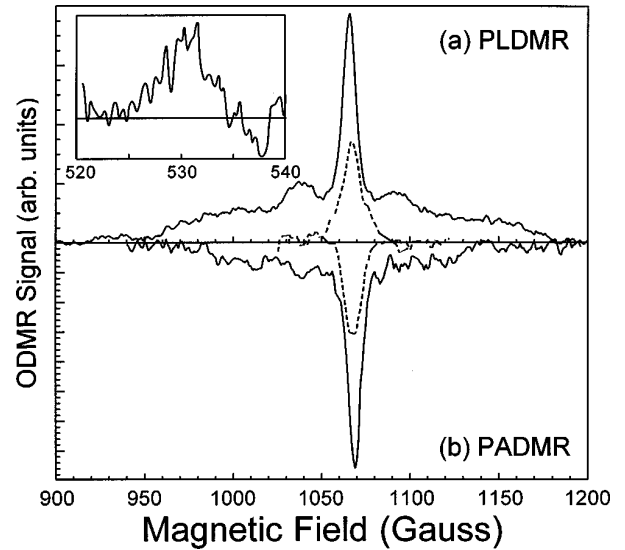


FIG. 3. (a) H -PLDMR and (b) H -PADMR spectra of pristine (dashed line) and 10 mol % C_{60} -doped (solid line) DOO-PPV. Inset: half-field polaron pair PLDMR spectrum.

correlated with the ~ 70 -G-wide resonance, which rules out magnetic dipole interactions.^{26,30} We show below that this resonance can be explained by an isotropic spin exchange interaction between two dissimilar polarons.

DOO-PPV is a promising π -conjugated polymer, which has a high quantum yield¹⁵ and shows little evidence of polaron pair formation. However, we can induce polaron pair formation by fullerene doping.²¹ Charge transfer from the polymer chain to C_{60} creates a high steady-state population of PPV^+/C_{60}^- pairs³¹ and results in quite dramatic changes to the PLDMR spectrum. The H -PLDMR and H -PADMR spectra of pristine and 10 mol % C_{60} :DOO-PPV from 900 to 1200 G are shown in Fig. 3. Both spectra contain a spin- $\frac{1}{2}$ resonance at 1072 G; the PLDMR of the doped sample is roughly 10 times as intense as that of the undoped sample. The most striking difference between the two spectra is the appearance of a ~ 200 -G-wide resonance about $g \approx 2$ with clearly resolved shoulders at 1045 and 1095 G, respectively. In addition, a weak “half-field” PLDMR signal appears at 530 G in doped DOO-PPV shown in the inset of Fig. 3.

There are several possible explanations for the observed broad (~ 200 G) resonant spectrum (BRS) around $g \approx 2$ and its accompanying “half-field” resonance. This excitation must have spin 1 (or no half-field resonance) and cannot be triplet excitons native to PPV as the BRS is much narrower than that previously observed by ODMR.^{32,33} The observed BRS does resemble that of photoexcited C_{60} triplets,³⁴ but this explanation is problematic. The PL of the composite film is due to emission from singlet excitons on DOO-PPV. Hence, any excitation on C_{60} could only indirectly influence the PL. Moreover, magnetic resonant enhancement of ${}^3C_{60}$ decay would lead to the creation of more PPV^+/C_{60}^- defect centers, yielding a PL-quenching resonance, not an enhancing one. Spin-correlated polaron pairs can explain the BRS feature and its “half-field” companion. For a fullerene-polymer blend, the PPV^+ polaron could be bound to either a PPV^- polaron on the polymer chain or a C_{60}^- molecule. We have not observed a similar resonance in pure DOO-PPV; it

is therefore reasonable to suggest that the BRS and its half-field companion are due to bound P^+/C_{60}^- complexes.

B. Model

In Figs. 2 and 3, we attributed two distinct kinds of magnetic resonance spectra to exchange interactions. The polaron pair ODMR spectrum of DBO-PPE has no half-field resonance, whereas the pair spectrum of C_{60} :DOO-PPV has both full- and half-field resonances. These cases result from isotropic and anisotropic exchange interactions, respectively. For an exchange coupled pair of polarons, the spin Hamiltonian is written as

$$H_{S-S} = g_e \mathbf{H} \cdot \mathbf{S}_e + g_h \mathbf{H} \cdot \mathbf{S}_h + H_{ex}, \quad (2)$$

where $\mathbf{S}_{e,h}$ are the spins of the positive and negative polarons, the gyromagnetic tensors \vec{g}_e and \vec{g}_h are assumed to be isotropic, and \mathbf{H} is the magnetic field. The exchange Hamiltonian is $H_{ex} = \mathbf{S}_e \cdot \vec{J} \cdot \mathbf{S}_h$, where \vec{J} is the exchange tensor. The exchange tensor can be decomposed into the sum of a traceless, symmetric tensor \vec{D}_J , and an antisymmetric tensor \vec{A}_J : $\vec{J} = \vec{I} + \vec{D}_J + \vec{A}_J$, where $J = \frac{1}{3}\text{Tr}(\vec{J})$ and \vec{I} is the identity matrix. Using this decomposition, the exchange Hamiltonian can then be written as

$$H_{ex} = JS_e \cdot \mathbf{S}_h + \mathbf{S}_e \cdot \vec{D}_J \cdot \mathbf{S}_h + \mathbf{d} \cdot \mathbf{S}_e \times \mathbf{S}_h, \quad (3)$$

where \mathbf{d} is an axial vector. If the two polarons are related to one another by a center of inversion symmetry, there is no antisymmetric term.¹⁷

1. Isotropic exchange interaction

We first consider an isotropic exchange interaction ($J_x = J_y = J_z$). In this case, the spin Hamiltonian can be written as

$$H_{S-S} = g_e \mathbf{H} \cdot \mathbf{S}_e + g_h \mathbf{H} \cdot \mathbf{S}_h + JS_e \cdot \mathbf{S}_h. \quad (4)$$

This Hamiltonian has the following eigenstates and eigenvalues:^{35,36}

$$|1\rangle = |+, +\rangle, \quad E_1 = \bar{g}\beta H + J/4,$$

$$|2\rangle = \cos \theta |-, +\rangle + \sin \theta |-, +\rangle, \quad E_2 = -J/4 + \frac{1}{2} \sqrt{J^2 + (\delta g \beta H)^2},$$

$$|3\rangle = -\sin \theta |-, +\rangle + \cos \theta |-, +\rangle, \quad E_3 = -J/4 - \frac{1}{2} \sqrt{J^2 + (\delta g \beta H)^2},$$

$$|4\rangle = |-, -\rangle, \quad E_4 = -\bar{g}\beta H + J/4,$$

where $\delta g = |g_e - g_h|$, $\bar{g} = (g_e + g_h)/2$, and $2\theta = \arctan(J/\delta g \beta H)$. Figure 4(a) shows the energies of these levels for $g\beta H \gg J$ and $J > 0$. The transition rate R_{ij} between two coupled states is $R_{ij} = |\langle i | H_{\mu\text{wave}} | j \rangle|^2$,³⁷ where $H_{\mu\text{wave}}$ is the microwave perturbation. If the microwave magnetic field $\mathbf{H}_1 \perp \mathbf{H}$, $H_{\mu\text{wave}} = g_e \mu_B S_{ex} + g_h \mu_B S_{hx}$. If $g_e = g_h$, the eigenvalues of $|2\rangle$ are $S=1$ and $m_S=0$ and the eigenvalues of $|3\rangle$ are $S=0$ and $m_S=0$. The only allowed transitions are then $|1\rangle \rightarrow |2\rangle$ and $|4\rangle \rightarrow |2\rangle$, which occur at the field $H_0 = h\nu/g\beta$. However, if $g_e \neq g_h$, $|2\rangle$ and $|3\rangle$ have mixed S

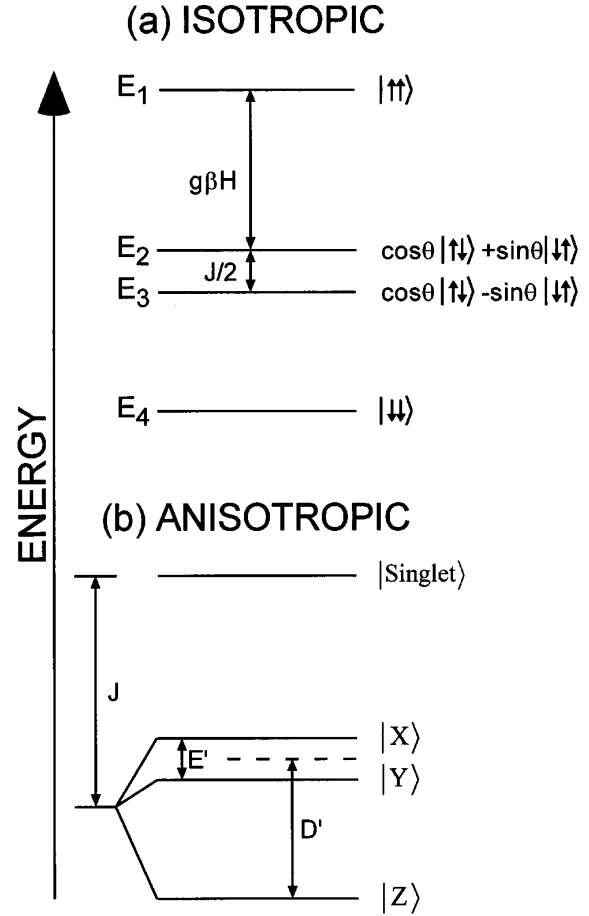


FIG. 4. Schematic diagram of polaron pair energy levels with (a) isotropic or (b) anisotropic exchange interactions.

$=0$ and $S=1$ character. Then, instead of the two-line spectrum associated with the two polarons, the exchange spectrum of the polaron pair contains four lines. The transition fields and amplitudes for our system ($H_0 = 1070$ G) are plotted in Fig. 5 as a function of J . The two outer lines ($|1\rangle \rightarrow |3\rangle$ and $|4\rangle \rightarrow |3\rangle$), associated with triplet-singlet transitions, move further away from H_0 and rapidly weaken as J increases. It is important to note that the “half-field” transition ($|1\rangle \rightarrow |4\rangle$) is *strictly forbidden* for an isotropic spin exchange interaction.

Figure 6(a) shows a simulated ODMR spectrum resulting from an isotropic exchange interaction with $J=20$ G between a pair of dissimilar ($g_e \neq g_h$) polarons. We take into account the g value of the polarons, generation and recombination rates for each spin sublevel, and the width of the polaron resonance itself. In most conjugated polymers, contributions from the negative and positive polarons cannot be resolved. We therefore take $\delta g \beta H \cong 1$ G, which corresponds to g values of 2.001 and 2.003, respectively, for the interacting positive and negative polarons. For the isotropic spin exchange interaction to result in a significant broadening of the polaron resonance, population differences among the triplet sublevels must be much smaller than population difference between triplet and singlet levels. In other words, $|N_{1,4} - N_2| \ll |N_{1,4} - N_3|$, where N_i is the steady-state population of the spin sublevel $|i\rangle$. For example, the recombination rates of triplet sublevels may be much slower than that of the singlet sublevel. This leads to high steady-state triplet

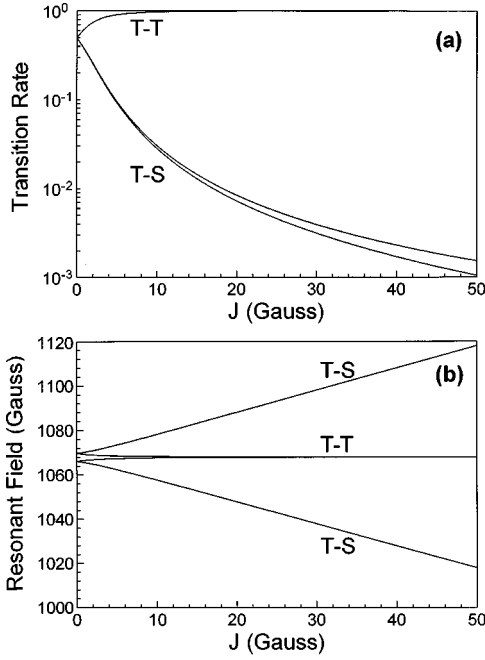


FIG. 5. Magnetic resonance (a) transition rates and (b) resonant fields for an isotropic exchange interaction and 3-GHz microwaves. Triplet-triplet (T - T) ($|1\rangle, |4\rangle \rightarrow |2\rangle$) and triplet-singlet (T - S) ($|1\rangle, |4\rangle \rightarrow |3\rangle$) transitions are marked.

sublevel populations and the desired spin polarization. Finally, the spectrum in Fig. 6(a) assumes a Gaussian line shape with a full width at half maximum of $\Delta H = 10$ G, which is typical for π -conjugated polymers.

The best fit to the H -PADMR spectrum of DBO-PPE [Fig. 6(b)] cannot be obtained with single values of J and ΔH . Whereas the simulation exhibits two distinct satellites,

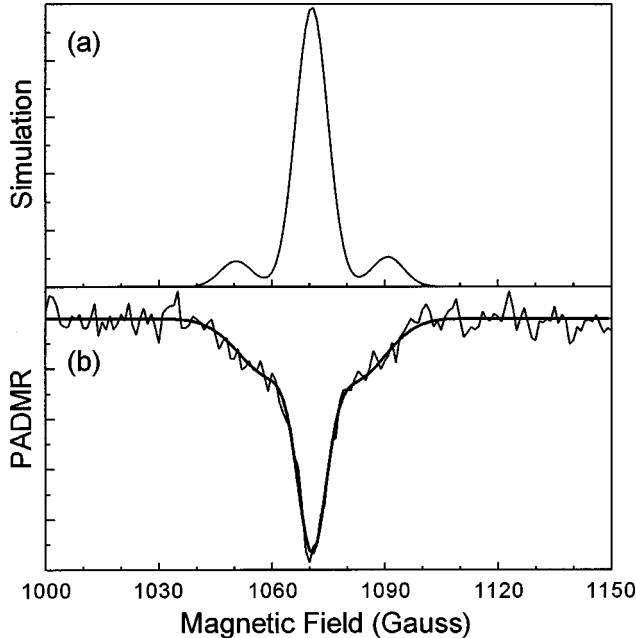


FIG. 6. (a) Simulated magnetic resonance spectrum of polaron pair with isotropic $J = 20$ G and a Gaussian linewidth $\Delta H = 10$ G. (b) Simulated and experimental PADMR spectra of polaron pairs in DBO-PPE from Fig. 2.

the polaron pair ODMR spectrum of DBO-PPE is featureless. The strength of the exchange interaction is proportional to the overlap integral of the polaron wave functions and is given by $J = J_0 e^{-2r/r_0}$, where r is the radius of the pair and r_0 and J_0 are determined by the inherent strength of the exchange interaction.^{35,38} This broadening reflects the distribution of J due to varying polaron pair distances. We simulated the PADMR spectrum of DBO-PPE [dashed line, Fig. 6(b)] with a single value of J (12 G), but setting the broadening of the satellite bands $\Delta H_{\text{sat}} = 20$ G. Because of the inherent width of the ODMR spectrum, it would be difficult to determine the actual distribution of J .

2. Anisotropic exchange interaction

We now relax the condition that the exchange interaction be isotropic. As long as $\delta g \beta H \ll J$, the spin Hamiltonian can be written as³⁶

$$H_{SS} = g_e \mathbf{H} \cdot \mathbf{S}_e + g_h \mathbf{H} \cdot \mathbf{S}_h + J \mathbf{S}_e \cdot \mathbf{S}_h + \mathbf{S}_e \cdot \vec{D}_J \cdot \mathbf{S}_h$$

$$= \bar{g} \beta H m_S + J[S^2 - 3/2] + \frac{1}{2}(J'_x S_x^2 + J'_y S_y^2 + J'_z S_z^2), \quad (5)$$

where S and m_S are the usual spin quantum numbers and $J'_x = J_x - J$, etc. Equation (5) has an even (singlet) solution at $E_S = -\frac{3}{4}J$ and three odd (triplet) solutions centered at $E_T = \frac{1}{4}J$. As \vec{D}_J is traceless, H_{SS} can be written in terms of two independent parameters $D' = \frac{3}{4}J'_z$ and $E' = \frac{1}{4}(J'_x - J'_y)$. D' and E' are referred to as the zero-field splitting (ZFS) parameters due to the exchange interaction. The spin Hamiltonian ${}^3H_{SS}$ for the odd solutions now reads

$${}^3H_{SS} = \bar{g} \beta H m_S + J[S^2 - 3/2] + D'(S_z^2 - \frac{1}{3}S^2) + E'(S_x^2 - S_y^2). \quad (6)$$

This spin Hamiltonian has the same form as that of a regular triplet exciton with a singlet-triplet splitting of J and ZFS parameters D' and E' . Due to this similarity, it would be difficult to distinguish between triplet powder patterns due to magnetic dipole interactions from those due to spin-exchange interactions. ${}^3H_{SS}$ has three triplet solutions, $|X\rangle, |Y\rangle, |Z\rangle$, for the three principal axes of the exchange triplet. These energy levels are shown schematically in Fig. 4(b).

The anisotropic spin exchange interaction mixes the triplet sublevels, permitting both $\Delta m_s = \pm 1$ and $\Delta m_s = \pm 2$ transitions. Therefore, an exchange triplet powder pattern has both FF and HF powder pattern resonances. The FF powder pattern due to $\Delta m_s = 1$ transitions has the following critical points:³⁶

$$\text{singularities at } H = H_0 \pm (D' - 3E')/2, \quad (7a)$$

$$\text{shoulder at } H = H_0 \pm (D' + 3E')/2, \quad (7b)$$

$$\text{and steps at } H = H_0 \pm D'. \quad (7c)$$

The HF powder pattern due to $\Delta m_s = 2$ microwave transitions consists of

$$\text{a singularity at } H = \frac{1}{2}H_0 \sqrt{1 - [(D+E)/H_0]^2} \quad (8a)$$

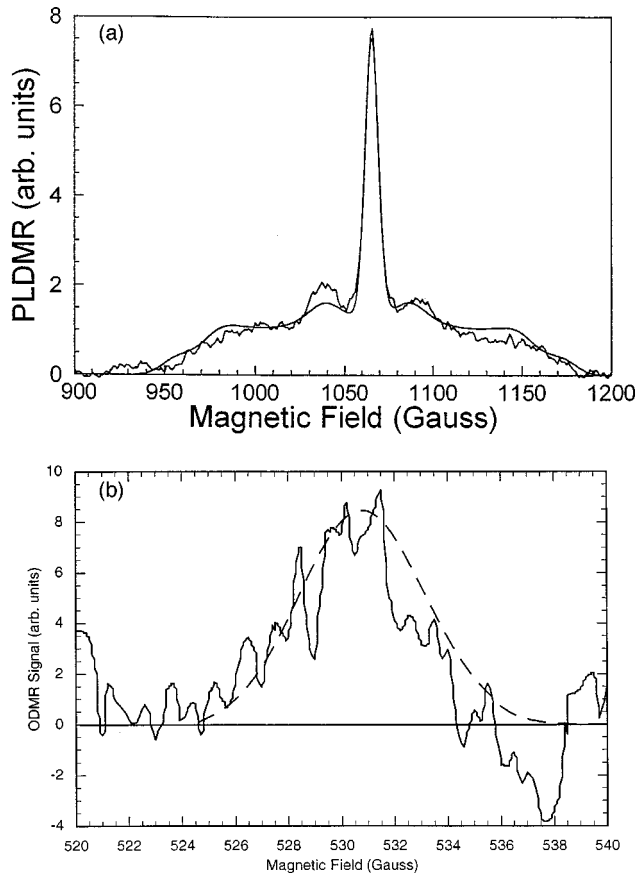


FIG. 7. Simulated anisotropic exchange powder pattern and PLDMR of C_{60} -doped DOO-PPV from Fig. 3. Inset: Simulated and experimental results at half field.

and a shoulder at $H = \frac{1}{2}H_0\sqrt{1 - [(D-E)/H_0]^2}$. (8b)

We simulated the magnetic resonance spectrum of C_{60} :DOO-PPV by adding a Gaussian line at $g=2$ due to noninteracting polarons to an anisotropic spin exchange triplet powder pattern with ZFS parameters $D' = 122$ G and $E' = 15$ G. Figure 7 shows the simulation is in good agreement with the experimental data.

IV. SPECTRAL SIGNATURE OF POLARON PAIRS

A. λ -PADMR spectra of DBO-PPE and C_{60} :DOO-PPV

Having identified polaron pairs by a spin exchange interaction, we can now use PA and λ -PADMR to measure their absorption spectra. The PA and λ -PADMR spectra of DBO-PPE are shown in Fig. 8. The PA spectrum consists of a weak band at 0.4 eV (PP_1) and strong PA above 1.2 eV with bands at 1.35, 1.55, and ≈ 1.75 eV, respectively. The bands at 0.4 and 1.75 eV correspond to the polaron pair λ -PADMR spectrum [Fig. 8(b)], measured at either the peak of the narrow line ($H = 1070$ G) or on the broad resonance ($H = 1050$ G) [Fig. 2(b)]. We note that the PP_2 band is much stronger than the PP_1 band. While the triplet resonance was too weak to directly measure its spectrum by λ -PADMR, C_{60} doping completely quenches the triplet PLDMR spectrum.²⁹ The resulting PA spectrum [Fig. 8(a)] contains the polaron pairs bands PP_1 and PP_2 and a weaker feature at

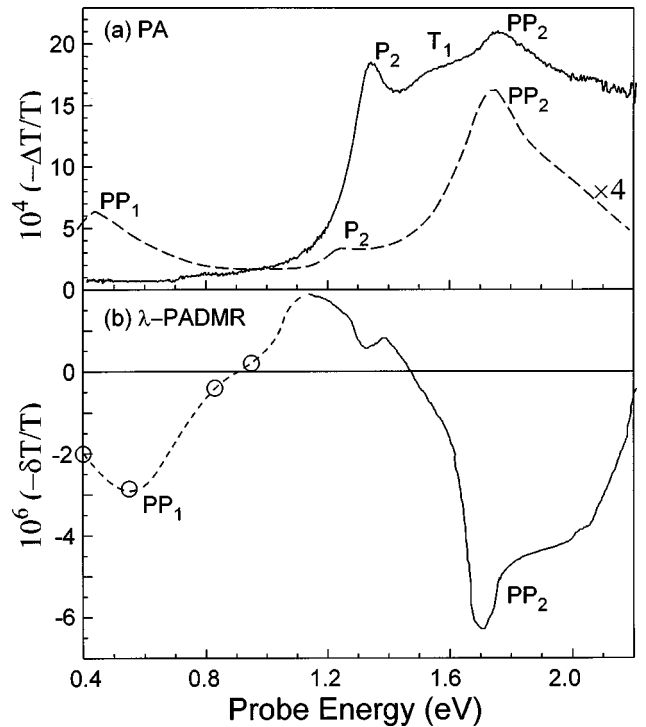


FIG. 8. (a) PA spectra of pure (solid line) and 1 mol % C_{60} -doped (dashed line) DBO-PPE. (b) λ -PADMR spectrum of DBO-PPE film measured at 1070 G. Transitions of polarons, polaron pairs, and triplet excitons are marked.

1.3 eV due to polarons (P_1). We therefore attribute the band at 1.6 eV to triplet excitons and the band at 1.35 eV to isolated polarons.

The H -PADMR of the 10% C_{60} :DOO-PPV sample is affected by the spin exchange interaction (Fig. 3), enabling us to separately measure the absorption spectra of isolated polarons at $H = 1072$ G and P^+/C_{60}^- complexes at $H = 1050$ G, respectively. These spectra are shown in Fig. 9 along with the PA and triplet λ -PADMR spectra. The po-

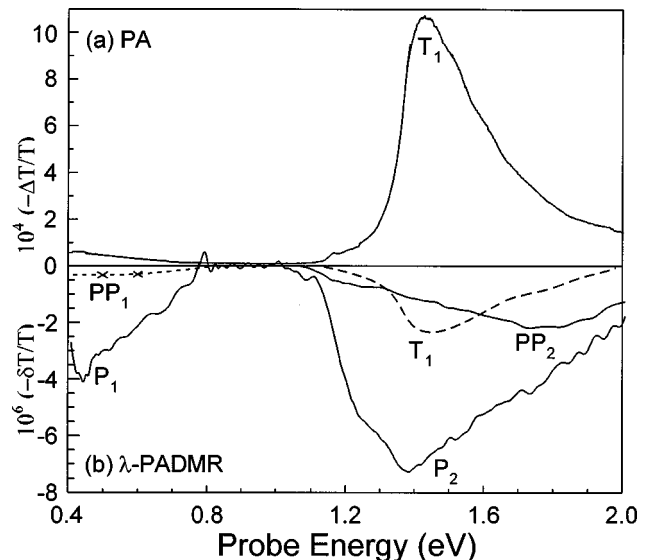


FIG. 9. (a) PA and (b) λ -PADMR spectra of 10 mol % C_{60} -doped DOO-PPV. The λ -PADMR spectra were taken at 400 G (triplet), 1050 G (polaron pair), and 1070 G (polaron), respectively.

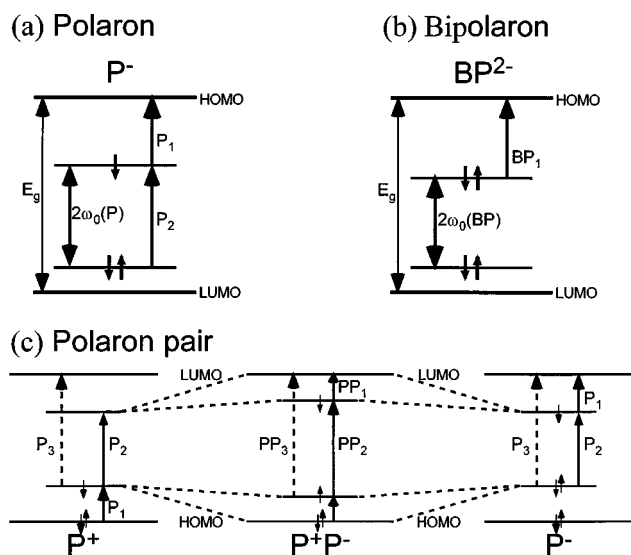


FIG. 10. Schematic diagram of polaron and polaron pair energy levels and their respective optical transitions.

laron λ -PADMR consists of two bands with maxima at 0.45 and 1.4 eV, respectively. The polaron pair λ -PADMR also contains two bands, labeled PP_1 and PP_2 as above. The PP_2 band is blueshifted by about 0.4 eV with respect to P_2 of isolated polarons and is much stronger than the PP_1 band. We do not see transitions of C_{60}^- molecules at 1.2 eV or their magnetic resonance at $g = 1.995$. The triplet λ -PADMR spectrum is the same as the PA spectrum itself, indicating that the PA spectrum is dominated by triplet excitons even at 10 mol % doping. This indicates that C_{60} doping of DOO-PPV is relatively weak.³⁹

We summarize the above results in Fig. 10 with a schematic diagram of the energy levels and optical transitions of polarons and polaron pairs. Both polarons and polaron pairs have two optical transitions; the polaron pair transition PP_2 occurs at a higher energy than the P_2 transition and the pair transition PP_1 is relatively weak. The shift of the energy levels is due to the Coulomb attraction between the oppositely charged polarons composing the pair. Mizes and Conwell¹¹ have shown that a Coulomb interaction between polarons composing the pair shifts the energy-level positions. Due to their mutual attraction, the energy levels of the negative polaron shift upwards and those of the positive polaron shift downwards. Mizes and Conwell predict three transitions; the highest-energy pair transition (PP_2) is blueshifted with respect to the high-energy P_2 transition. If the transition that transfers an electron between the partially occupied levels of the two polarons is weak or forbidden, their calculations are in agreement with our experimental results.

Our results may explain the PA bands observed in several ps transient measurements of films of PPV derivatives at energies around 1.8 eV.^{12,15,21,39,40} In good PPV films the transient PA spectrum shows a PA band of excitons at 1.5 eV whose dynamics match those of the PL and stimulated emission (SE).¹⁵ However, in measurements made at high excitation densities⁴⁰ or of oxidized¹² or C_{60} -doped^{15,21,39} films, there appears a new PA band at about 1.8 eV whose dynamics are not correlated with those of the PL and SE. Based on our λ -PADMR results here, we can safely attribute the new PA band at 1.8 eV to polaron pair excitations. These

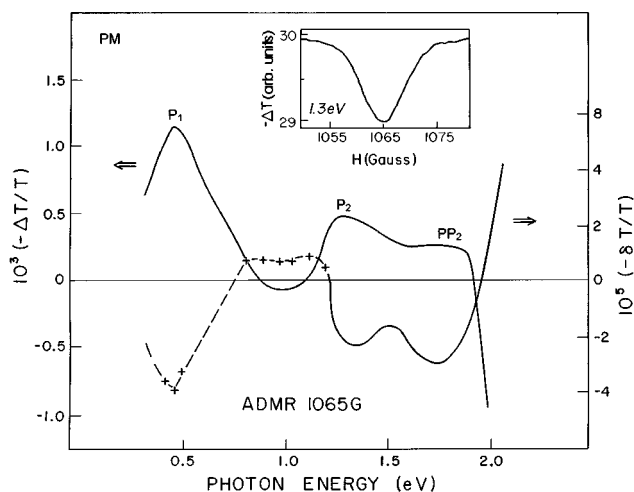


FIG. 11. (a) PA spectrum and (b) λ -PADMR spectrum measured at 1065 G of e -PT. Inset: H -PADMR spectrum at 1.3 eV.

may be created via exciton dissociation at extrinsic defects such as carbonyls¹² or photoinduced C_{60}/PPV^+ complexes³⁹ or by exciton-exciton annihilation at high excitation intensities.⁴⁰ This solves a puzzle in the field of photophysics in PPV that has recently been extensively debated.

B. Polaron pair spectra in other π -conjugated polymers

We generalize our results by considering several other systems that exhibit polaron pairs in their PA spectra. Electrochemically polymerized polythiophene (e -PT) is weakly luminescent ($\eta < 10^{-3}$), due to a high defect density.²³ The PA spectrum of e -PT is shown in Fig. 11(a). It contains three PA bands: P_1 at 0.45 eV, P_2 at 1.25 eV, and PP_2 at 1.8 eV, respectively.⁴¹ The transient PA spectrum [Fig. 12(a)] also contains three bands, one of which (PP_2) decays more quickly than the other two (P_1 and P_2). The dynamics of the three bands, measured at their peak energies [Fig. 12(b)], shows that P_1 and P_2 have fairly similar decays. We also note that the P_1 and P_2 bands are correlated with infrared active vibrations (IRAV's) whereas the PP_2 band is not.²³ Hence, the P_1 and P_2 bands must be associated with charged excitations, whereas the PP_2 band must be associated with neutral excitations.

The H -PADMR spectrum of e -PT, measured at the peak of the three PA bands, is shown in Fig. 11 inset. The H -PADMR is negative, contains a narrow resonance about $g = 2$ due to spin- $\frac{1}{2}$ excitations, but no spin-1 resonances. Hence, \vec{J} must be *isotropic*. The λ -PADMR spectrum of e -PT, measured at 1067 G and shown in Fig. 11(b), contains the same three bands as the PA spectrum, but with different relative intensities.⁴¹ The microwave-induced change in the photoexcitation density $\delta n/n$ is -3×10^{-2} for both P_1 and P_2 bands, whereas $\delta n/n$ is -7×10^{-2} for the PP_2 band. We also find a positive band, which we have recently shown⁴² is the signature of bipolarons. We assign the P_1 and P_2 bands to polarons and the $\delta n/n > 0$ λ -PADMR band to bipolarons. The band at 1.8 eV cannot be due to a third optical transition of polarons, as these should follow a sum rule of $P_1 + P_2 = P_3$.⁴³ The lack of a triplet PADMR rules out triplet excitons as its origin. We therefore suggest an assignment of

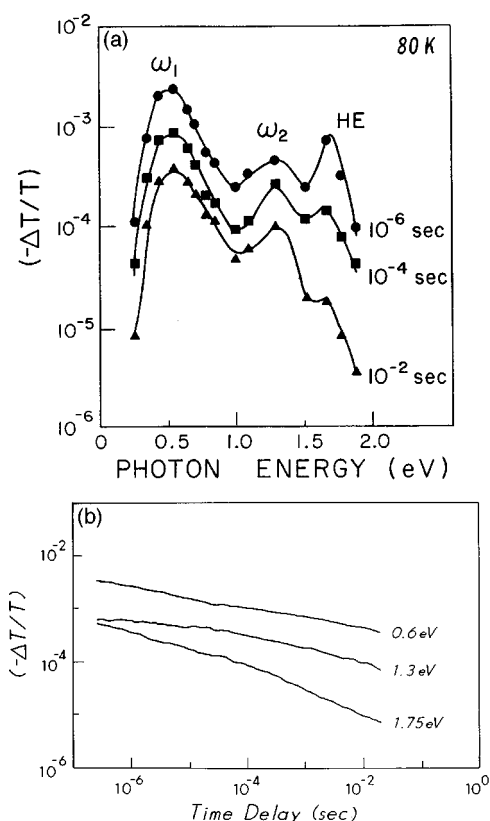


FIG. 12. (a) Transient PA spectrum of *e*-PT film as the pump-probe delay time is varied. (b) Dynamics of the polaron (P_1 and P_2) and polaron pair (PP_2) PA bands.

polaron pairs, most likely resulting from dissociation of singlet excitons at defect centers. This interpretation is consistent with the low PL quantum yield and high defect density in these films.

We have further evidence for this interpretation in examining the PA and λ -PADMR spectra of poly(3-octylthiophene). P3OT is different from *e*-PT in that it has a much higher PL efficiency ($\eta \approx 0.15$) and a strong triplet ODMR.^{25,28} The PA spectrum of P3OT, shown in Fig. 13(a), consists of a band at 0.5 eV and a much stronger band at 1.45 eV. The spin- $\frac{1}{2}$ λ -PADMR spectrum [Fig. 13(b)] shows that the band at 0.5 eV is the P_1 transition of polarons and reveals the P_2 band at 1.25 eV. As with *e*-PT, there is a positive λ -PADMR band at ≈ 1.1 eV, which we again assign to bipolarons.⁴² Comparison of the spin-1 λ -PADMR spectrum to the PA spectrum (Fig. 13) reveals that the band at 1.45 eV is due to transitions of triplet excitons. The spin- $\frac{1}{2}$ λ -PADMR also contains a band with a peak at 1.9 eV. We assign this band to the PP_2 transition of polaron pairs.

The PA spectrum of C_{60} -doped P3OT (Ref. 44) is in agreement with these assignments. Charge transfer quenches the PL and sharply increases the PC.^{45,46} The PA spectrum of C_{60} :P3OT, shown in Fig. 13(c), resembles that of *e*-PT (Fig. 11). The triplet PA is quenched and the resulting spectrum contains two PA bands due to optical transitions of polarons and a PA band due to polaron pairs. We accordingly make the following spectral assignments: P_1 at 0.4 eV and P_2 at 1.2 eV are due to isolated polarons and PP_2 at 1.75 eV is due to polaron pairs. Similar changes have been previously reported in the transient⁴⁷ and steady-state PA spectra of

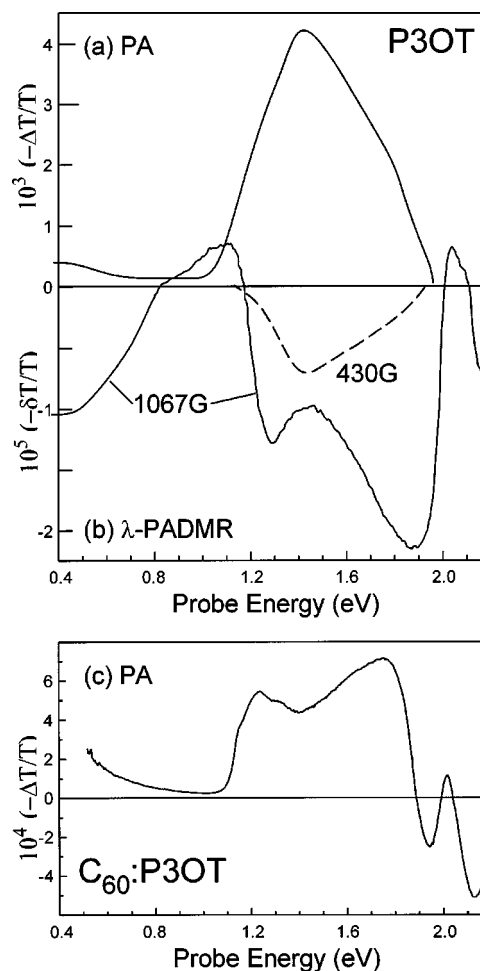


FIG. 13. (a) PA spectrum and (b) λ -PADMR spectrum measured at 1067 G of P3OT film. (c) PA spectrum of C_{60} -doped P3OT film.

MEH-PPV/ C_{60} (MEH denotes 2-methoxy-5-2'-ethylhexyloxy) composites.³³ Our results suggest that the blue-shift of the PA spectrum of MEH-PPV upon C_{60} doping is due to formation of polaron pairs.

PDES is a polymer with a somewhat unique character. The morphology of the repeat unit suggests that this material has a degenerate ground state. However, in experiment, PDES films have been found to contain chain segments with both short and long conjugation lengths. While the long segments do indeed have degenerate ground states, the shorter segments have degenerate ground states. Thus, excitations in these shorter segments consists of polarons, polaron pairs, and excitonic states. The PA spectrum (Fig. 14) appears to be dominated by these shorter segments; it consists of three bands at 0.35, 1.0, and 1.5 eV, respectively. Two of these bands are correlated with each other and with IRAV's below 0.2 eV. We thus identify these bands as the signature of polarons. The third PA band at 1.6 eV is then due to polaron pairs.

V. SPIN AND SPECTRAL SIGNATURES OF NEUTRAL SOLITON PAIRS IN POLYACETYLENE

The occurrence of paired excitations is not unique to polymers with nondegenerate ground states. The PM spectrum of trans-(CH)_x, shown in Fig. 15(a),²⁶ consists of two

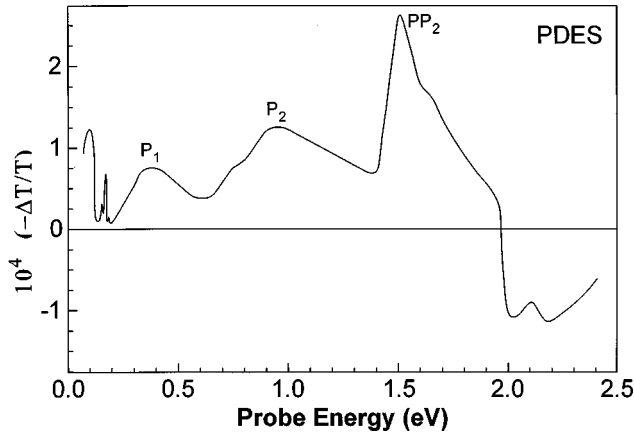
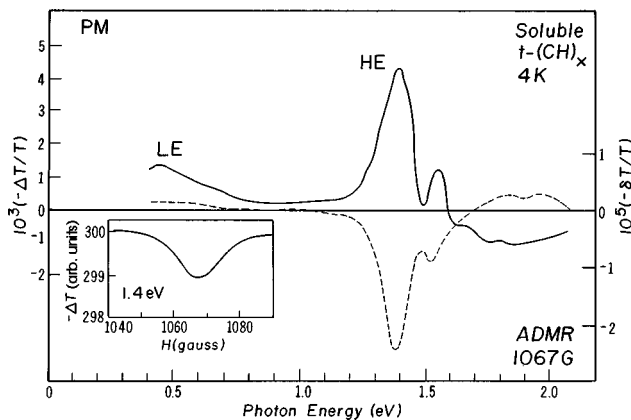
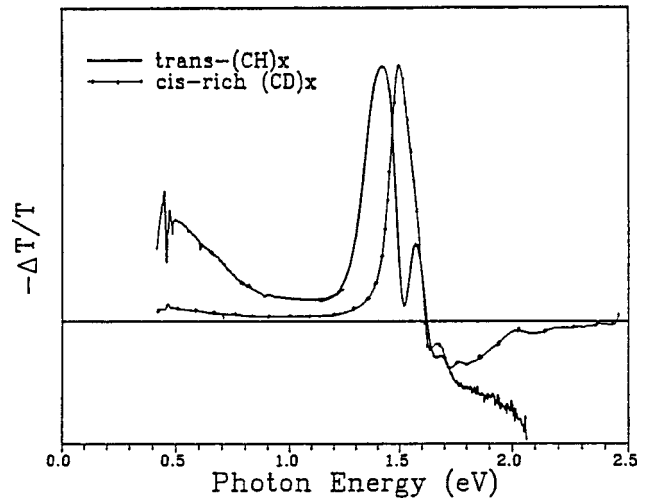


FIG. 14. PA spectrum of PDES film.

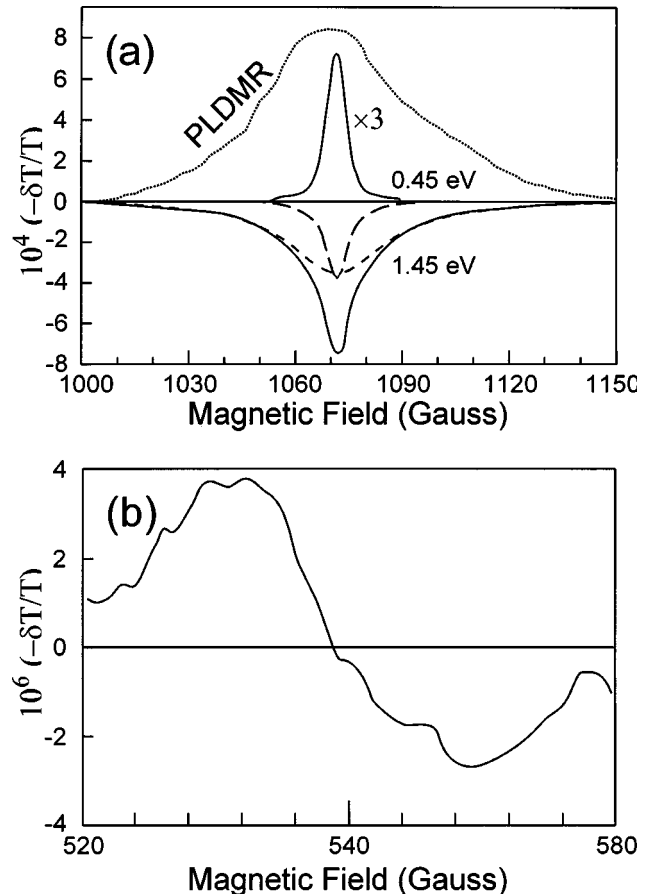
main PA bands and photobleaching above $h\nu > 1.6$ eV. The low-energy (LE) band peaks at 0.43 eV; its correlation with IRAV's requires that it originates from charged excitations. The intensity of the LE band saturates with increased excitation power and is sample dependent.²³ This band is now considered to originate from transitions of charged solitons, which are pushed away from mid-gap due to electron correlation.²⁸ The high-energy (HE) band, however, is not correlated with IRAV's and must therefore be due to an overall neutral state. This band does not depend upon sample treatment nor does it saturate at high excitation intensity. It is therefore intrinsic to the $(\text{CH})_x$ chain. The photobleaching has the same line shape as the absorption and is due to depletion of the ground-state population by laser excitation.

PADMR can conclusively determine the origin of the two PA bands. The λ -PADMR spectrum of $\text{trans}-(\text{CH})_x$, measured at $H = 1067$ G, is shown in Fig. 14(b). Both bands are correlated with spin- $\frac{1}{2}$ resonances, but have opposite signs. The H -PADMR line shape is Lorentzian, with a FWHM of 16.3 G (Fig. 14 inset). The two PADMR bands have identical PADMR line shapes and the same dependence on pump intensity and temperature dependence, indicating that they are correlated. The PA and H -PADMR spectra can be explained²⁸ by assigning the HE band to neutral soliton-antisoliton pairs and the LE band to charged solitons and antisolitons. Magnetic resonance enhances the decay of the neutral soliton-antisoliton pairs, resulting in a negative reso-

FIG. 15. PA and λ -PADMR spectra of $\text{trans}-(\text{CH})_x$ film. Inset: H -PADMR spectrum at 1.35 eV.FIG. 16. PA spectrum of cis-rich $(\text{CD})_x$ film.

nance measured at the HE band and a positive resonance measured at the LE band. The LE band is then due to charged solitons, which are spinless and have a single absorption band.^{26,28}

We find direct evidence for an exchange interaction between neutral solitons in short trans segments in cis-rich $(\text{CD})_x$. The PA spectrum of cis-rich $(\text{CD})_x$, shown in Fig.

FIG. 17. (a) Full-field and (b) half-field H -PADMR and H -PLDMR spectra of exchange-coupled soliton pairs in cis-rich $(\text{CD})_x$ film. The 1.45 eV H -PADMR is decomposed into broad and narrow resonances, shown as dashed lines.

16,⁴⁸ contains two PA bands: a weak (LE) band at 0.5 eV and an intense (HE) band at 1.49 eV. The PLDMR spectrum and *H*-PLDMR spectra of the two PA bands are shown in Fig. 17. The PADMR was measured between 1.3 and 1.5 eV, which Lauchmann *et al.*¹⁹ and Yoshino *et al.*⁴⁹ have shown is due to short trans segments in the film. The spin- $\frac{1}{2}$ *H*-PADMR of the HE band contains two δn contributions: a narrow line with a FWHM of ~ 8 G and a broader line with FWHM of ~ 32 G. Comparing their response to the microwave modulation frequency shows that these two lines have different dynamics. The λ -PADMR (at $g \approx 2$) spectrum of the broad line is also slightly blueshifted (0.04 eV) with respect to the narrow band.⁴⁸ The *H*-PADMR spectrum also contains a much weaker half-field feature; this feature has a derivative line shape with a zero crossing at 538 G [Fig. 17(b)]. The *H*-PADMR spectrum of the LE band shows only the narrow line whereas the PLDMR (Fig. 17, dotted line) contains the broad line and its half-field companion. Taken together, all of these data indicate the existence of two distinct states, both of which are related to spin- $\frac{1}{2}$ excitations. We assign the narrow component of the *H*-PADMR spectrum to isolated neutral solitons in long trans-(CH)_x chains and assign the broad line and its half-field companion to exchange coupled soliton pairs in short trans-(CH)_x chains.

VI. SUMMARY

We have studied the optical properties of polarons and polaron pairs in nondegenerate ground-state polymers and solitons and soliton pairs in trans-polyacetylene. These results are summarized in Table II. An exchange resonance broadens the spin- $\frac{1}{2}$ ODMR associated with polarons; both isotropic and anisotropic exchange interactions have been observed. An isotropic exchange interaction results in a broadening of the spin- $\frac{1}{2}$ resonance associated with polarons, whereas an anisotropic exchange interaction will give rise to

TABLE II. Optical transition energies (in eV) of polarons and polaron pairs.

| Polymer | P_1 | P_2 | PP ₁ | PP ₂ |
|--------------|---------|--------|------------------|-----------------|
| PDES | 0.35 eV | 1.0 eV | | 1.5 eV |
| <i>e</i> -PT | 0.45 | 1.25 | | 1.8 |
| P3OT | 0.4 | 1.2 | | 1.75 |
| DOO-PPV | 0.45 | 1.4 | ≈ 0.4 eV | 1.8 |
| DBO-PPE | | 1.35 | 0.4 | 1.75 |

both full-field and half-field powder patterns. Both interactions have been successfully modeled by incorporating the parameters of the exchange interaction and generation and recombination rates for each magnetic sublevel. PADMR spectroscopy has enabled us to directly measure the absorption spectra of polaron pairs; both polaron and polaron pairs have two PA bands. The PP₂ PA band of polaron pairs is blueshifted with respect to the P_2 PA band of isolated polarons and much stronger than the PP₁ band. We have also identified the PA bands of isolated solitons in long trans-(CH)_x segments and coupled soliton pairs in short trans-(CD)_x segments.

ACKNOWLEDGMENTS

We would like to thank our collaborators for useful discussions and generously providing the many samples used in this study: M. Ozaki and K. Yoshino for DOO-PPV, Y.-W. Ding and T. J. Barton for PDES and DBO-PPE, J. Poplowski and E. Ehrenfreund for *e*-PT, and D. Moses for P3OT, trans-(CH)_x, and cis-rich (CD)_x. We would also like to thank J. Shinar and M. Liess for assistance with measurements on DBO-PPE and C₆₀:P3OT, respectively. This work was supported in part by the Department of Energy under Grant No. FG03-96-ER45490.

*Present address: The University of Sheffield, Sheffield S3 7RH, United Kingdom.

†Present address: Los Alamos National Laboratory, Los Alamos, New Mexico.

¹J. H. Burroughes *et al.*, Nature (London) **347**, 539 (1990).

²For a review of recent advances, see Proceedings of the International Conference on Synthetic Metals, Seoul, S. Korea, 1994, edited by Y. W. Park and H. Lee [Synth. Met. **69–71** (1995)]; Proceedings of the International Conference on Synthetic Metals, Salt Lake City, UT, 1996, edited by Z. V. Vardeny and A. J. Epstein [Synth. Met. **85** (1997)].

³I. D. W. Samuel, B. Crystall, G. Rumbles, P. L. Burn, A. B. Holmes, and R. H. Friend, Chem. Phys. Lett. **213**, 472 (1993).

⁴N. T. Harrison, G. R. Hayes, R. T. Phillips, and R. H. Friend, Phys. Rev. Lett. **77**, 1881 (1996).

⁵P. Gomes da Costa and E. M. Conwell, Phys. Rev. B **48**, 1993 (1993).

⁶Z. Shuai, J. L. Brédas, and W. P. Su, Chem. Phys. Lett. **228**, 301 (1994).

⁷M. Chandross, S. Mazumdar, S. Jeglinski, X. Wei, Z. V. Vardeny, E. W. Kwok, and T. M. Miller, Phys. Rev. B **50**, 14 702 (1994).

⁸B. Mollay, U. Lemmer, R. Kersting, R. F. Mahrt, H. Kurz, H. F.

Kauffmann, and H. Bässler, Phys. Rev. B **50**, 10 769 (1994).

⁹S. Heun, R. F. Mahrt, A. Greiner, U. Lemmer, H. Bäsler, D. A. Halliday, D. D. C. Bradley, P. L. Burns, and A. B. Holmes, J. Phys., Condens. Matter **5**, 247 (1993).

¹⁰R. Kersting, U. Lemmer, R. F. Mahrt, H. Kurz, H. Bässler, and E. O. Göbel, Phys. Rev. Lett. **70**, 3820 (1993).

¹¹H. A. Mizes and E. M. Conwell, Phys. Rev. B **50**, R11243 (1994).

¹²M. Yan, L. J. Rothberg, E. W. Kwock, and T. M. Miller, Phys. Rev. Lett. **75**, 1992 (1995); Synth. Met. **80**, 41 (1996).

¹³J. Fagaström and S. Strafström, Phys. Rev. B **54**, 13 713 (1996).

¹⁴N. C. Greenham, I. D. W. Samuel, G. R. Hayes, R. T. Phillips, Y. A. R. R. Kessener, S. C. Moratti, A. B. Holmes, and R. H. Friend, Chem. Phys. Lett. **241**, 89 (1995).

¹⁵S. Frolov, Ph.D. thesis, University of Utah, 1996 (unpublished); S. Frolov *et al.* (unpublished).

¹⁶E. L. Frankevich, A. A. Lymarev, I. Sokolik, F. E. Karasz, S. Blumstengel, R. H. Baughman, and H. H. Hörhold, Phys. Rev. B **46**, 9320 (1992).

¹⁷A. Bencini and D. Gatteschi, *EPR of Exchange Coupled Systems* (Springer-Verlag, Berlin, 1990).

¹⁸C₆₀ obtained from the MER Corporation.

¹⁹L. Lauchmann, S. Etemad, T. C. Chung, A. J. Heeger, and A. G.

- MacDiarmid, Phys. Rev. B **24**, 3701 (1981).
- ²⁰Z. V. Vardeny, E. Ehrenfreund, J. Shinar, and F. Wudl, Phys. Rev. B **35**, RC2498 (1987).
- ²¹N. S. Sariciftci and A. J. Heeger, Int. J. Mod. Phys. B **8**, 237 (1994).
- ²²Y. Ding, Ph.D. thesis, Iowa State University, 1992 (unpublished).
- ²³X. Wei, Ph.D. thesis, University of Utah, 1992 (unpublished).
- ²⁴M. Sharnoff, J. Chem. Phys. **46**, 3263 (1967).
- ²⁵A. L. Kwiram, Chem. Phys. Lett. **1**, 272 (1967).
- ²⁶X. Wei, B. C. Hess, Z. V. Vardeny, and F. Wudl, Phys. Rev. Lett. **68**, 666 (1992).
- ²⁷L. S. Swanson, J. Shinar, and K. Yoshino, Phys. Rev. Lett. **65**, 1140 (1990).
- ²⁸X. Wei and Z. V. Vardeny, *Handbook of Conducting Polymers II* (Marcel Dekker, New York, 1997), Chap. 22.
- ²⁹The PLDMR spectrum was measured on a spectrometer operating at 9.35 GHz with a resonant field of ≈ 3.35 kG. These measurements were described in greater detail in P. A. Lane, J. Shinar, and K. Yoshino, Phys. Rev. B **54**, 9308 (1996) and Ref. 30.
- ³⁰P. A. Lane, Ph.D. thesis, Iowa State University, 1994 (unpublished).
- ³¹The steady-state excitation density N_{SS} of any excitation is given by the relation $N_{SS} = G\eta\tau$ where G is the generation rate per cubic cm, η is the quantum yield, and τ the excitation lifetime. For our system, $G = 6 \times 10^{23} \text{ cm}^{-3} \text{ s}^{-1}$. If we assume a unit quantum yield for exciton dissociation and an excitation lifetime of $\tau > 1$ ms below 100 K, we find $N_{SS} \geq 6 \times 10^{21} \text{ cm}^{-3}$. This actually exceeds the density of fullerene molecules in the film.
- ³²L. S. Swanson, P. A. Lane, J. Shinar, and F. Wudl, Phys. Rev. B **44**, 10 617 (1991).
- ³³X. Wei, Z. V. Vardeny, N. S. Sariciftci, and A. J. Heeger, Phys. Rev. B **53**, 2817 (1996).
- ³⁴P. A. Lane, L. S. Swanson, Q. X. Ni, J. Shinar, J. P. Engel, T. J. Barton, and L. Jones, Phys. Rev. Lett. **68**, 887 (1992).
- ³⁵F. Boulitroup, Phys. Rev. B **28**, 6192 (1983).
- ³⁶A. Abragan and B. Bleaney, *Electron Paramagnetic Resonance of Transition Metal Ions* (Clarendon, Oxford, 1970).
- ³⁷E. Fermi, *Nuclear Physics* (University of Chicago Press, Chicago, 1950), p. 142.
- ³⁸P. W. Anderson, Solid State Phys. **14**, 99 (1983).
- ³⁹P. A. Lane, M. Liess, X. Wei, S. Frolov, Z. V. Vardeny, and Z. H. Kafafi, *Fullerenes and Photonics III*, SPIE Proceedings No. 2854 (SPIE, Bellingham, 1996), p. 102.
- ⁴⁰D. W. McBranch and M. B. Sinclair, in *The Nature of the Photoexcitations in Conjugated Polymers*, edited by N. S. Sariciftci (World Scientific Publishing, Singapore, 1997), Chap. 20, and references therein.
- ⁴¹G. S. Kanner, X. Wei, B. C. Hess, L. R. Chen, and Z. V. Vardeny, Phys. Rev. Lett. **69**, 538 (1992).
- ⁴²P. A. Lane, X. Wei, and Z. V. Vardeny, Phys. Rev. Lett. **76**, 1544 (1996).
- ⁴³K. Fesser, A. R. Bishop, and D. K. Campbell, Phys. Rev. B **27**, 4804 (1983).
- ⁴⁴M. Liess and Z. V. Vardeny (unpublished).
- ⁴⁵S. Morita, A. A. Zakhidov, and K. Yoshino, Solid State Commun. **82**, 249 (1992).
- ⁴⁶S. Morita, S. Kiyomatsu, A. A. Zakhidov, and K. Yoshino, J. Phys., Condens. Matter. **4**, L103 (1992).
- ⁴⁷N. S. Sariciftci, L. Smilowitz, A. J. Heeger, and F. Wudl, Science **258**, 1474 (1992).
- ⁴⁸X. Wei, Z. V. Vardeny, E. Ehrenfreund, D. Moses, and Y. Cao, Synth. Met. **54**, 321 (1993).
- ⁴⁹K. Yoshino, S. Hayashi, T. Sakai, Y. Inuishi, H. Kato, and Y. Watanabe, Jpn. J. Appl. Phys. **21**, 1653 (1982); Solid State Commun. **46**, 583 (1983).